Cation coordination by calix[4]arenes bearing amide and/or phosphine oxide pendant groups: how many arms are needed to bind Li^+ *vs.* Na^+? A combined NMR and molecular dynamics study

Marc Baaden,[a] Georges Wipff,[a] Mohamed Reza Yaftian,[b] Michel Burgard[b] and Dominique Matt[c]

[a] *Laboratoire MSM, Institut de Chimie, Université Louis Pasteur, UMR CNRS 7551, 4, rue Blaise Pascal, F-67070 Strasbourg Cedex, France*
[b] *Laboratoire de Chimie Minérale et Chimie Physique Industrielle, ECPM, Université Louis Pasteur, UMR CNRS 7512, 25, rue Becquerel, F-67087 Strasbourg Cedex, France*
[c] *Groupe de Chimie Inorganique Moléculaire, Université Louis Pasteur, UMR CNRS 7513, 1, rue Blaise Pascal, F-67008 Strasbourg Cedex, France*

Received (in Cambridge, UK) 24th December 1999, Accepted 18th May 2000
Published on the Web 15th June 2000

Combined spectroscopic and theoretical studies have been performed on two recently developed calix[4]arenes in the cone conformation, **L1** (bearing two $-CH_2C(O)NEt_2$ and two $-CH_2P(O)Ph_2$ substituents occupying respectively distal phenolic positions) and **L2** (with four $-CH_2P(O)Ph_2$ substituents), in order to compare the Li^+ *vs.* Na^+ cation binding mode. Molecular dynamics simulations indicate that coordination of the Li^+ cation involves three of the four substituents (the two phosphoryl groups and one of the two amide functions of **L1**; three phosphoryl arms of **L2**). A variable temperature NMR study carried out with **L1**·Li^+ confirms this fourfold coordination and reveals that in solution the lithium cation moves between the two adjacent $O_PO_PO_{amide}$ units. The weaker binding of the Na^+ cation results in a more symmetrical coordination of the four phenolic oxygen atoms and two carbonyls of **L1** or four phosphoryls of **L2**.

Introduction

Calix[4]arenes substituted at the lower rim by several amide,[1–3] ester[4–6] or phosphoryl ligands[7–11] are effective cation binders in homogeneous solution as well as in liquid–liquid extraction systems. Many of these modified calixarenes show a marked affinity for hard cations.[12] The binding properties mainly rely on the capability of their oxygen binding sites to delineate a pseudocavity suitable for cation encapsulation. This picture is consistent with recently reported X-ray structures, *e.g.* that of the *p-tert*-butylcalix[4]arene–$\{OCH_2C(O)NEt_2\}_4$·KSCN complex where the potassium ion sits in a fourfold symmetrical environment consisting of four carbonyl units and four phenolic oxygen atoms.[13,14] To the best of our knowledge, no X-ray data are available for phosphoryl-containing calixarene analogues. Whether such inclusive structures are retained in solution is unclear, due to possible competition between solvation of the binding sites and cation coordination. As previously shown by molecular dynamics (MD) simulations on *p-tert*-butylcalix[4]arenetetradiethylamide complexes, a water environment leads to a dynamic exchange between converging and diverging orientations of the binding sites, while in a less polar solvent like acetonitrile the structures are close to those found in the solid state.[15] Whether the structures of complexes with a given cation are representative of those with a cation of different size is another matter of concern, in particular for small ions like Li^+. Again, MD simulations on the *p-tert*-butylcalix[4]arenetetradiethylamide Li^+ complex showed that three arms, instead of four, are sufficient to bind Li^+. In addition to *endo* complexes, more loosely bound *exo* ones may be present in solution.[15] In the case of M^{3+} lanthanide complexes of *p-tert*-butylcalix[4]arene fitted with four pendant $O–CH_2–(Me_2)P=O$ arms, versatile binding modes have been characterised, depending on the stoichiometry, the solvent and counterion effects.[11]

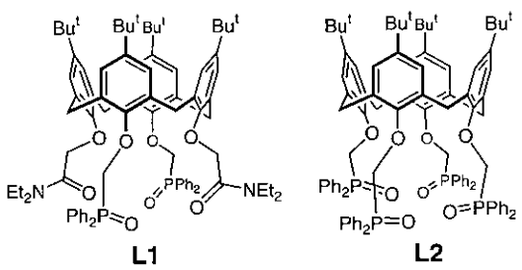

Fig. 1 The mixed diamide–diphosphine oxide calix[4]arene **L1** and the tetrasubstituted phosphine oxide ligand **L2**.

The present work deals with structural aspects of Na^+ and Li^+ binding using two recently synthesised *p-tert*-butylcalix[4]arene derivatives, namely **L1** and **L2** (Fig. 1). Ligand **L1** is substituted at the lower rim by two amide and two phosphoryl arms while **L2** contains four phosphoryl pendant groups. As inferred from extraction experiments in weakly polar diluents such as *e.g.* dichloroethane or tetrahydrofuran, both ligands form 1:1 complexes with alkali ions.[8] The present study is aimed at answering the following questions: how many arms of each ligand are involved in cation coordination? Does the cation bind equally to these arms, or do some binding groups coordinate more strongly? Is the coordination static, or does it dynamically exchange between several forms?

DOI: 10.1039/b000019l

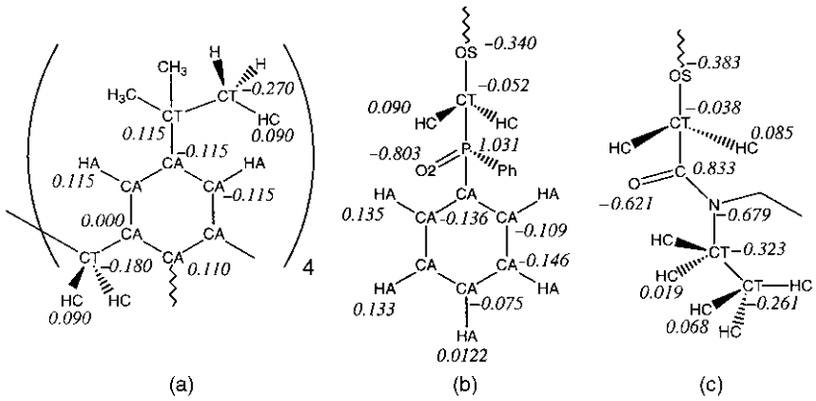

Fig. 2 AMBER atom types and atomic charges used for the cone (a), phosphine oxide (b) and amide (c) fragments of calixarenes **L1** and **L2**.

Methods

^{1}H and ^{31}P NMR spectra were recorded on an ARX 500 Bruker instrument (500 MHz). The ^{1}H NMR spectral data were referenced to residual protiated solvent (δ 7.26, $CDCl_3$ or δ 5.32, CD_2Cl_2), and the ^{31}P data are reported relative to external H_3PO_4. The IR spectrum of [**L1**·Li]BF_4 was recorded on a Perkin-Elmer 1600 spectrometer (4000–400 cm^{-1}). The mass spectrum of [**L1**·Li]BF_4 was recorded on a ZAB HF VG analytical spectrometer using tetraglyme as matrix.

Preparation of [L1·Li]BF_4

[**L1**·Li]BF_4 was prepared by addition of dry lithium tetrafluoroborate (0.0105 g, 0.11 mmol) to a dichloromethane solution (25 mL) of **L1** (0.1304 g, 0.1 mmol). After stirring for 24 h, the solution was filtered and concentrated under reduced pressure. Addition of *n*-hexane resulted in formation of a white precipitate which was dried under vacuum. IR (KBr and nujol): 1658 ($\nu_{C=O}$) cm^{-1}. ^{1}H-NMR (500 MHz, $CDCl_3$, −50 °C): δ 7.99–7.95, 7.66–7.62, 7.49–7.46 and 7.29–7.27 (m, 20H, PPh_2), 7.02 (s, 2H, *m*-Ar*H*), 6.60 and 4.61 (ABX spin system, X = P, 4H, $OCH_2P(O)Ph_2$), ^2J(AB) = 16 Hz, ^2J(PA) = 8 Hz, ^2J(PB) = 8 Hz; δ 6.57 (s, 2H, *m*-ArH); δ 6.51 (s, 2H, *m*-ArH); δ 5.85 (s, 2H, *m*-ArH), 4.23 and 4.08 (2s, 4H, $OCH_2C(O)NEt_2$), 4.18 and 3.28 (AB spin system, 4H, $ArCH_2Ar$, ^2J = 7 Hz), 3.96 and 2.48 (AB spin system, 4H, $ArCH_2Ar$, ^2J = 13 Hz), 3.67 (q, 2H, NCH_2CH_3, ^4J = 7 Hz), 3.11 (q, 2H, NCH_2CH_3, ^4J = 7 Hz), 2.98 (q, 4H, NCH_2CH_3, ^4J = 7 Hz), 1.36 (t, 3H, NCH_2CH_3, ^3J = 7 Hz), 1.25 (s, 18H, Bu^t), 1.14 and 1.03 (2t, 6H, NCH_2CH_3, ^3J = 7 Hz), 0.89 (s, 9H, Bu^t), 0.75 (t, 3H, NCH_2CH_3, ^3J = 7 Hz), 0.47 (s, 9H, Bu^t); ^{31}P ($CDCl_3$, −30 °C, relative to H_3PO_4 85% as external reference): δ 32.2. FAB ms (ZAB HF VG Analytical, tetraglyme): 1309.7 (100%, $[M - BF_4]^+$). Anal. Calcd. for $C_{82}H_{100}BF_4N_2O_8P_2Li$: C, 70.48; H, 7.21; N, 2.00. Found: C, 70.26; H, 7.08; N, 2.06%. **L1**·Na^+ was prepared using a procedure similar to that outlined above, but using $NaBF_4$ as alkali salt. ^{1}H-NMR (500 MHz, $CDCl_3$, −50 °C): δ 7.54–7.49 and 7.37–7.32 (m, 20H, PPh_2), 6.88 (br s, 4H, *m*-ArH), 6.64 (br s, 4H, *m*-ArH), 5.10 (s, 4H, OCH_2), 4.74 (s, 4H, OCH_2), 4.46 and 3.13 (br AB spin system, 8H, $ArCH_2Ar$), 3.57 (q, 4H, NCH_2, ^3J = 7 Hz), 3.28 (q, 4H, NCH_2, ^3J = 7 Hz), 1.37 (t, 6H, NCH_2CH_3, ^3J = 7 Hz), 1.25 (t, 6H, NCH_2CH_3, ^3J = 7 Hz), 1.08 (s, 18H, Bu^t), 1.07 (s, 18H, Bu^t). Compound [**L2**·Li]BF_4 (synthesis similar to that of [**L1**·Li]BF_4): ^{1}H-NMR (500 MHz, CD_2Cl_2, −70 °C): δ 7.97–7.06 (m, 40H, PPh_2), δ 6.72–6.64 (br s, 8H, *m*-ArH), 5.09 (s, 8H, PCH_2), 4.16 and 2.63 (br AB spin system, 8H, $ArCH_2Ar$), 0.92 (s, 36H, Bu^t). ^{31}P ($CDCl_3$, −50 °C, 202.5 MHz): δ 35.0. Compound [**L2**·Na]BF_4 (synthesis similar to that of [**L1**·Li]BF_4): ^{1}H-NMR (500 MHz, CD_2Cl_2, −25 °C): δ 7.80–7.29 (m, 40H, PPh_2), 6.49 (s, 8H, *m*-ArH), 5.10 (s br, 8H, PCH_2), 4.26 and 2.66 (AB spin system, 8H, ^2J = 12.8 Hz, $ArCH_2$), 0.96 (s, 36H, Bu^t).

Crystallisation of [L1·Na]BF_4. Crystals of [**L1**·Na]BF_4 were obtained by slow diffusion of heptane into a chlorobenzene solution containing stoichiometric amounts of **L1** and $NaBF_4$.

Crystal data for [L1·Na]BF_4.† $C_{171}H_{216}B_2F_8N_4Na_2O_{16}P_4$, M = 2927.13, monoclinic, space group $P2_1/c$, colorless crystals, a = 27.739(1), b = 24.1268(5), c = 12.2940(5) Å, β = 92.051(6)°, U = 8222.5(8) Å^3, Z = 2, D_c = 1.18 g cm^{-3}, μ = 0.122 mm^{-1}, $F(000)$ = 3124. Data were collected on a Nonius KappaCCD diffractometer (graphite Mo-Kα radiation, 0.71073 Å) at −100 °C. 19248 Reflections collected ($2.5 \le \theta \le 27.47°$), 9213 data with $I > 3\sigma(I)$. The structure was solved using the Nonius OpenMoleN package[16] and refined by full matrix least-squares with anisotropic thermal parameters for all non-hydrogen atoms. Final results: $R(F)$ = 0.058, $wR(F)$ = 0.081, goodness of fit = 1.485, 921 parameters, largest difference peak = 0.541 e Å^{-3}.

Molecular dynamics (MD)

The simulations were performed using the AMBER4.1 sofware[17] and program suite.[18,19] The potential energy function U includes bond, angle and dihedral terms and pairwise additive 1-6-12 (electrostatic and van der Waals) interactions of the Lennard-Jones type between non-bonded atoms:

$$U = \Sigma_{bonds}\, K_r\,(r - r_{eq})^2 + \Sigma_{angles}\, K_\theta(\theta - \theta_{eq})^2 + \Sigma_{dihedrals}\Sigma_n V_n(1 + \cos n\varphi) + \Sigma_{i<j}\,[q_iq_j/R_{ij} - 2\varepsilon_{ij}(R_{ij}^*/R_{ij})^6 + \varepsilon_{ij}(R_{ij}^*/R_{ij})^{12}]$$

Atom type parameters were taken from the AMBER force field[20] as in previous studies on calix[4]arenes.[3,15,21] The atomic charges of the cone moiety of the calixarenes (Fig. 2a) are taken from CHARMM.[22] Those of the phosphine oxide and amide fragments (Fig. 2b and 2c, respectively) were fitted with SPARTAN[23] from ESP calculations at the RHF level using a 6-31G* basis set. The Li^+ and Na^+ cation parameters are those from Åqvist.[24]

All inclusive **L**·M^+ complexes have been simulated by MD *in vacuo* at 300 K. Some of them were also simulated in chloroform solution explicitly represented at the same temperature, and at 500 K in the gas phase. Details are given in Table 1. Each calculation was run for at least 1 ns in the thermodynamic NVT ensemble at 300 K.

Results

Variable temperature NMR study on [L1·Li]BF_4

In order to get some insight into the coordinative properties of

† CCDC reference number 188/251. See http://www.rsc.org/suppdata/p2/b0/b000019l/ for crystallographic files in .cif format.

Table 1 Simulation conditions for $L \cdot M^+$ *in vacuo* (temperature and simulation time) and in chloroform solution (temperature, simulation time, number of solvent molecules and box size in Å^3)

Solute	*T*/K	Time/ns	Number $CHCl_3$	Box size $V_x \times V_y \times V_z$
L1·Li^+	300, 500	1.0	—	
L1·Na^+	300, 500	1.0	—	
L2·Li^+	300, 500	1.0	—	
L2·Na^+	300, 500	1.0	—	
L1·Li^+	300, 500	1.0	345	36.8 × 36.7 × 36.7

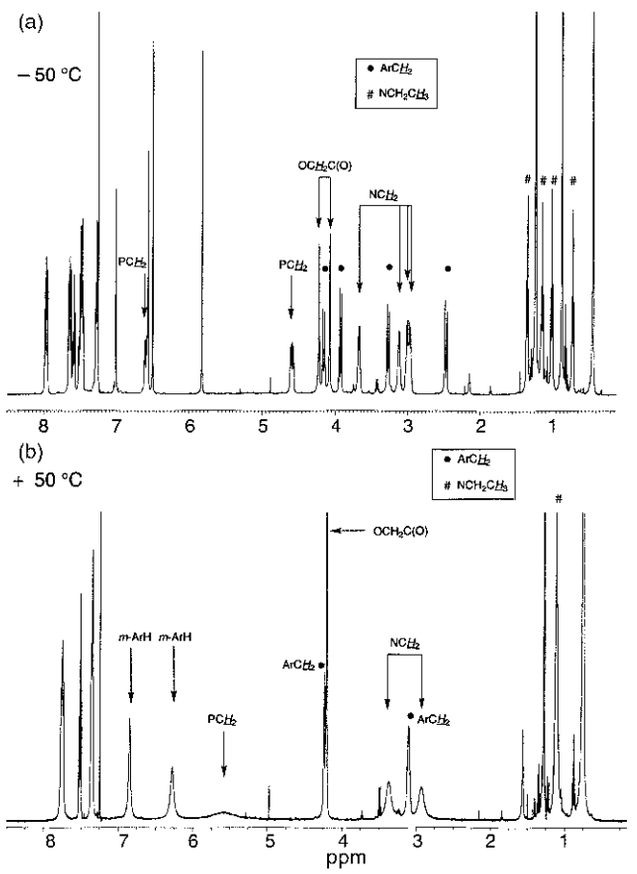

Fig. 3 NMR spectra of [**L1**·Li]BF_4 at −50 °C (a, top) and at +50 °C (b, bottom) in $CDCl_3$.

L1 towards the lithium ion we undertook a variable temperature NMR study on [**L1**·Li]BF_4. A pure sample of this complex was prepared by reaction of **L1** with one equiv. of $LiBF_4$ in CH_2Cl_2 (see Experimental section). The ^{1}H-NMR spectrum (500 MHz, $CDCl_3$) of [**L1**·Li]BF_4 measured at −50 °C displays sharp signals (Fig. 3a) and reveals the following patterns: (*i*) two AB spin systems for the ArCH_2Ar groups (relative intensity 1 : 1); (*ii*) three signals for *tert*-butyl groups with relative intensities of 1 : 1 : 2; (*iii*) a single ABX spin system due to the PCH_2 groups (δ_A 6.60, δ_B 4.61 ppm); (*iv*) four *m*-Ar*H* signals of equal intensity (at 7.02, 6.57, 6.51 and 5.58 ppm); (*v*) two distinct amide groups. These data are fully consistent with a C_s-symmetrical structure where the lithium cation is bonded to two phosphoryl groups and only one amide. Note, the low temperature ^{31}P-NMR spectrum (−30 °C, 202.5 MHz) which shows a single peak at 32.2 ppm (*cf*. 23.7 ppm for the free ligand) corroborates these observations. By increasing the temperature (Fig. 3b) most ^{1}H-NMR signals broadened; the signals due to the PCH_2 atoms, for example, coalesce at 20 °C, and above this temperature merge into a single A_2X pattern (X = P). Similarly, at higher temperatures (+50 °C; Fig. 3b), the two amides become equivalent on the NMR timescale. These observations can be interpreted in terms of fast exchange between the free and coordinated amide groups, with both phosphoryl groups remaining attached to the metal centre. Possibly, these dynamics are also accompanied by a slight shift of the lithium ion with respect to the calix platform, the lithium being alternatively bonded to the two possible sets of one amide and two phosphine oxide arms (Scheme 1). When these experiments were

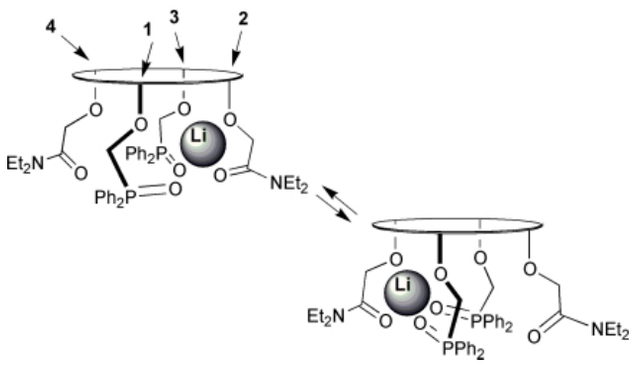

Scheme 1 Proposed dynamics for **L1**·Li^+. The numbering scheme for the pendant arms will be used in the text.

repeated at a 10-fold lower concentration, no significant changes were found for the coalescence temperatures, in keeping with an intramolecular exchange phenomenon. Using the Eyring equation,[25] an activation barrier of about 53 ± 2 kJ mol^{-1} was found for the exchange process. The ^{1}H NMR spectrum (500 MHz) at −50 °C of the sodium analogue [**L1**·Na]BF_4 displays C_{2v} symmetry, hence indicating a symmetrically bonded Na atom. For the tetraphosphorylated complexes [**L2**·Li]BF_4 and [**L2**·Na]BF_4, the ^{1}H NMR spectra are fully consistent with C_4 symmetrical structures at temperatures above −70 °C (500 MHz, CD_2Cl_2), and −25 °C, respectively. Thus alkali complexation involving only three pendant groups could only be evidenced in the case of [**L1**·Li]BF_4.

Molecular dynamics study of M·L1$^+$ and M·L2$^+$ complexes

Schematically, the cation may bind to the oxygen binding sites (O_C/O_P) of the calixarene arms, as well as to the phenolic O_{ph} oxygen atoms. Most of the complexes display dynamic features and cation coordination patterns. Typical average structural and energy features obtained at 300 K are summarised in Table 2.

We first analyze the mixed calixarene **L1** containing two distal amides and two distal phosphoryl arms. In the gas phase, the **L1**·Li^+ and **L1**·Na^+ complexes display a marked difference in cation binding mode. Two binding modes were tested and used as a starting configuration: one, where the cation was initially coordinated to either 2 O_P and 1 O_C oxygens, the other with a coordination by 1 O_P and 2 O_C oxygens. After 1 ns of dynamics on **L1**·Li^+, both modes converged to two structure types, where three arms only wrap around the cation. The first one (M1) corresponds to a four-coordinated cation which is nearly equidistant from the two O_P atoms (at 1.9 Å), one O_C (at 2.0 Å) and from the phenolic O_{ph} oxygen of the coordinated amide arm (at 2.2 Å; see Fig. 4a). In the second type of structure (M2), Li^+ binds to two O_C atoms and one O_P oxygen (at about 2.0 Å), complemented by weaker dynamic interactions with all four O_{ph} oxygen atoms (at about 2.8 Å). Thus, in the first type of complex Li^+ sits at a somewhat higher position with respect to the calixarene reference plane.[26] Its stability is higher than that of M2 by about 6 kcal mol^{-1} and involves a tighter cation binding. It also corresponds to smaller fluctuations of the $M^+ \cdots O$ distances. In both cases, the cone of **L1** is elongated and highly asymmetrical, two opposite aromatic units being nearly perpendicular, while the two others, involving the

Table 2 Mean $M^+ \cdots O$ distances and energy components and their fluctuations in different $L \cdot M^+$ complexes, at 300 K *in vacuo* and in chloroform solution. Two binding modes M1 and M2 are investigated for Li^+

	L1					**L2**	
	in chloroform		*in vacuo*			*in vacuo*	
M^+	Li^+		Li^+		Na^+	Li^+	Na^+
Binding mode	$2O_P + 1O_C$	$1O_P + 2O_C$	$2O_P + 1O_C$	$1O_P + 2O_C$		$3O_P$	$4O_P$
	Cation–Oxygen[a] distance/Å						
$M^+ \cdots O{=}P^1$	*1.89 ± 0.05*	4.71 ± 0.28	*1.90 ± 0.05*	4.71 ± 0.29	3.39 ± 1.11	5.47 ± 0.45	*2.34 ± 0.11*
$M^+ \cdots O{=}X^2$	*2.00 ± 0.08*	*2.00 ± 0.08*	6.27 ± 0.74	*2.01 ± 0.09*	*2.53 ± 0.30*	*1.90 ± 0.06*	*2.34 ± 0.10*
$M^+ \cdots O{=}P^3$	*1.90 ± 0.05*	*1.99 ± 0.09*	*1.89 ± 0.05*	*1.99 ± 0.09*	2.98 ± 0.93	*1.89 ± 0.05*	*2.34 ± 0.10*
$M^+ \cdots O{=}X^4$	7.01 ± 0.86	*2.06 ± 0.12*	*2.00 ± 0.08*	*2.06 ± 0.12*	2.77 ± 0.69	*1.89 ± 0.05*	*2.34 ± 0.10*
$M^+ \cdots O_{ph1}$	3.80 ± 0.36	2.63 ± 0.34	3.76 ± 0.31	2.80 ± 0.51	*2.64 ± 0.22*	6.04 ± 0.28	3.41 ± 0.35
$M^+ \cdots O_{ph2}$	*2.17 ± 0.15*	2.69 ± 0.39	5.67 ± 0.36	2.60 ± 0.42	*2.63 ± 0.22*	2.93 ± 0.34	3.39 ± 0.35
$M^+ \cdots O_{ph3}$	3.81 ± 0.29	2.98 ± 0.29	3.96 ± 0.27	2.86 ± 0.35	*2.62 ± 0.19*	4.38 ± 0.27	3.41 ± 0.35
$M^+ \cdots O_{ph4}$	5.60 ± 0.34	2.69 ± 0.39	*2.17 ± 0.17*	2.79 ± 0.42	*2.58 ± 0.22*	4.38 ± 0.28	3.40 ± 0.35
	Energy components/kcal mol^{-1}						
E LM^+	−9 ± 17	−4 ± 19	0.5 ± 7	6 ± 7	27 ± 7	244 ± 7	270 ± 7
E $M^+ \cdots L$	−178 ± 4	−177 ± 5	−178 ± 5	−182 ± 5	−154 ± 5	−186 ± 5	−170 ± 6
E $LM^+ \cdots$ chl	−132 ± 6	−133 ± 7	—	—	—	—	—

[a] $O{=}P^i$ are the phosphoryl oxygens. $O{=}X^i$ are the opposite amide oxygens in **L1** and the phosphoryl oxygens in **L2**. The index *i* refers to the numbering of the bonding arms as given in Scheme 1. O_{ph} are the phenolic oxygens. The values in italics correspond to coordinated oxygen atoms.

phenolic group bearing the unbound amide arm, are nearly parallel (Fig. 4a).

We checked that the models simulated *in vacuo* properly describe the complexes in chloroform solution. For this purpose, the **L1**·Li^+ complex was simulated for 1 ns in a bath of chloroform molecules, starting with the same two initial structures as in the gas phase. The average structures (Table 2) are, within statistical fluctuations, identical to those obtained in the gas phase. The energy difference between M2 and M1 binding modes is again about 5 kcal mol^{-1} in favour of the latter. As the solute–solvent interactions differ by less than 1 kcal mol^{-1} for both binding modes (Table 2), it can be concluded that gas phase results are representative of the behaviour of the complexes in chloroform solution and that the preferred mode of Li^+ binding involves two O_P's, one O_C, and the phenolic O_{ph} oxygen of **L1**, as shown in Scheme 1 and Fig. 4a.

When the **L1**·Li^+ system was simulated at higher temperature (500 K) in the gas phase for 1 ns, starting from a coordination of M1 type, the cation binding mode displayed a dynamic exchange between structures of this binding mode, the cation being most of the time instantaneously bound to three arms only. At about 400 ps, Li^+ migrated from one amide arm to the other, while remaining bonded to the two phosphoryl oxygens (Fig. 5).

In the case of the **L1**·Na^+ complex, the binding mode is different due to the larger size of the cation (Fig. 4b). The two simulations of 1 ns at 300 K which started with different cation binding modes rapidly converged to a unique type of complex, where the cone is of nearly fourfold symmetry, and the cation sits close to the symmetry axis, on the top of the four O_{ph} oxygens ($Na^+ \cdots O_{ph} = 2.6 \pm 0.2$ Å). In contrast to the Li^+ analogue, Na^+ is more tightly bound to the two O_C oxygens (at about 2.6 ± 0.5 Å) than to the two O_P's (at about 3.2 ± 1.0 Å). We also note that the $Na^+ \cdots O_P$ distances show larger fluctuations than the $Na^+ \cdots O_C$ ones, and that these fluctuations are much higher than in the corresponding Li^+ complex (Table 2). Comparison of the total energies of the Na^+ and Li^+ complexes shows that the latter is more stable (by about 27 kcal mol^{-1}), mostly due to the more favourable cation–ligand interaction energy.

The calixarene **L2** contains four identical phosphoryl arms which may, in principle, delineate a more regular pseudocavity than **L1**. Again, our MD simulations reveal different binding modes for Li^+ and Na^+, as illustrated by the average cation–oxygen distances reported in Table 2. Only three arms participate in the Li^+ binding (Fig. 4c), the corresponding O_P oxygens being strongly bound to the cation (at about 1.9 Å), whose coordination sphere is completed by one loosely bound O_{ph} oxygen (at about 2.9 Å). This contrasts with the Na^+ environment which is of fourfold symmetry (Fig. 4d) as confirmed by the $Na^+ \cdots O_P$ distances (Table 2). The Na^+ cation interacts strongly with the phosphoryl oxygen atoms (at about 2.3 ± 0.1 Å) and weakly with the O_{ph} ones (at about 3.4 ± 0.3 Å). Note also that the fluctuations of metal–oxygen distances in **L2**·Na^+ are smaller than those found for **L1**·Na^+ and **L2**·Na^+ is more rigid. In the **L2**·Na^+ complex, the calixarene cone has fourfold symmetry, while in **L2**·Li^+ it is elongated (Fig. 4c). Energetically the cation–ligand interaction energy is about 16 kcal mol^{-1} lower for Na^+ than for Li^+.

Solid state structure of the L1·Na^+ complex

An X-ray diffraction study (Fig. 6) carried out on [**L1**·Na]BF_4 shows that in the solid state the sodium ion is bonded to the four etheral ($Na \cdots O$ distances: 2.387(2), 2.413(2), 2.396(2), and 2.370(2) Å) and the two carbonyl oxygen atoms (2.305(3) and 2.282(2) Å). As anticipated by the MD calculations, the phosphoryl groups do not participate in bonding (distances *ca.* 4.08 and 3.82 Å). Whereas the cone of uncomplexed **L1** is of C_{2v} symmetry (with two opposite aromatic groups nearly parallel and the two others perpendicular)[27] it is of fourfold symmetry in the **L1**·Na^+ complex. The angle between opposite planes of aromatic groups is 125° between 1 and 3 (phosphine oxide), and 130° between 2 and 4 (amide; see numbering in Scheme 1). The CH_2 connectors of the cone form a square with sides of 5.1 Å length and diagonal distances of 7.20 and 7.24 Å. In the crystal, a heptane molecule "connects" two calixarenes *via* their hydrophobic upper rims. This is shown in Fig. 7. We note that the X-ray structure—determined at 173 K—is fully consistent with the mean MD simulated structure at 300 K (Table 2), taking into account the fluctuations of the dynamics. The experimental Na–O distances for bound oxygens are roughly 0.2–0.4 Å smaller, probably due to packing effects in the crystal and the reduced thermal motion at lower temperatures.

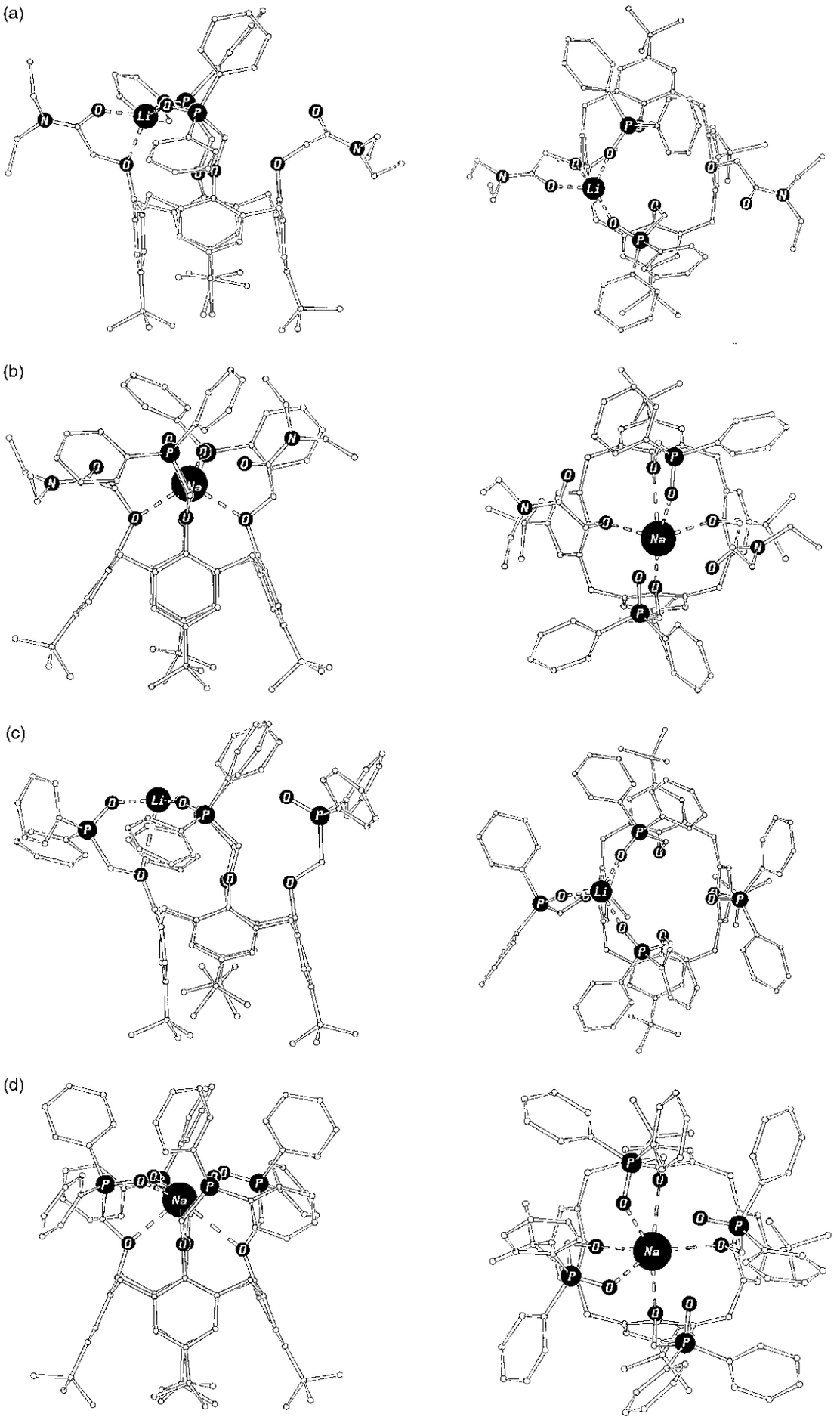

Fig. 4 Snapshots (orthogonal views) of the (a) **L1**·Li^+, (b) **L1**·Na^+, (c) **L2**·Li^+ and (d) **L2**·Na^+ complexes at the end of the simulations (1 ns).

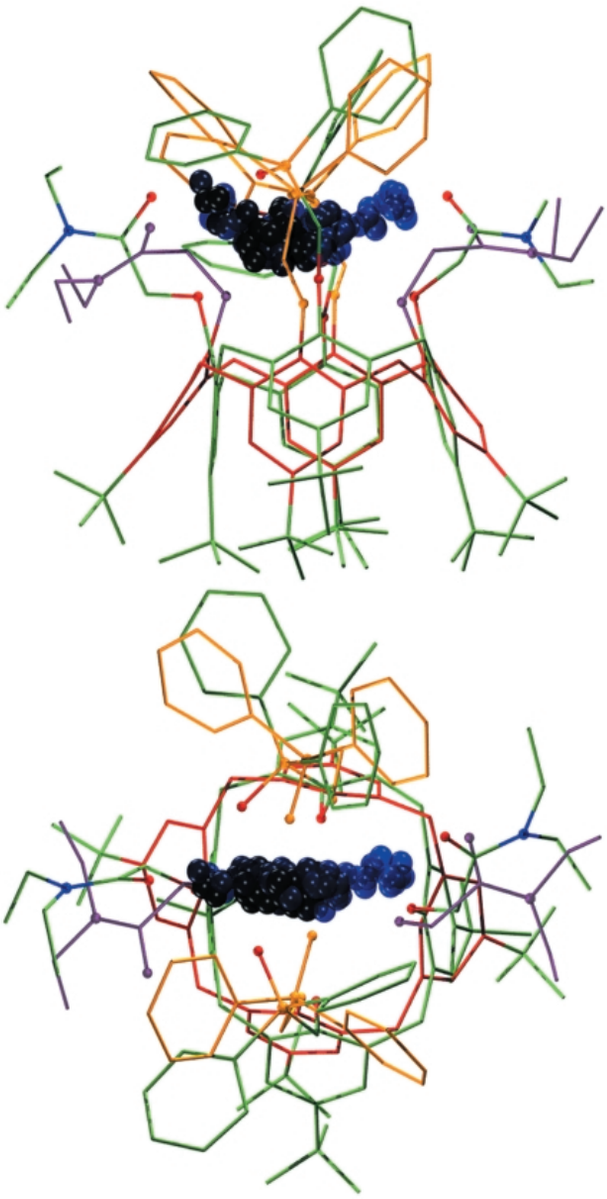

Fig. 5 Dynamics of the **L1**·Li^+ complex *in vacuo* at 500 K between 500 and 550 ps: cumulated Li^+ positions, initial and final structures of the ligand.

Discussion

Our simulations on **L1** and **L2** complexes indicate that the binding mode of the Li^+ cation involves three of the four calixarene arms only. In the case of **L1** this has been proven by variable temperature NMR experiments. For **L2** we could not evidence such behaviour, probably resulting from a significantly lower coalescence temperature, which was not accessible with the solvents used. Such a binding mode has already been mentioned earlier for related calixarenes,[15,16] and could be interpreted as a general trend due to the small ionic radius of Li^+. The MD simulations of the **L1**·Li^+ complex show a slight preference for a cation binding to two phosphoryl arms and to one of the amides (M1 binding mode). The discrimination between M1 and M2 binding modes is quite small. We believe that polarisation effects induced by the small and hard Li^+ cation would enhance the preference for the PO compared to the CO binding sites. Indeed, according to quantum mechanical calculations,[28] phosphoryl type ligands exhibit better binding energies than amide derivatives with M^{n+} cations (n = 1–3). For Na^+ the difference is approximately 5 kcal mol^{-1} per coordinated ligand.

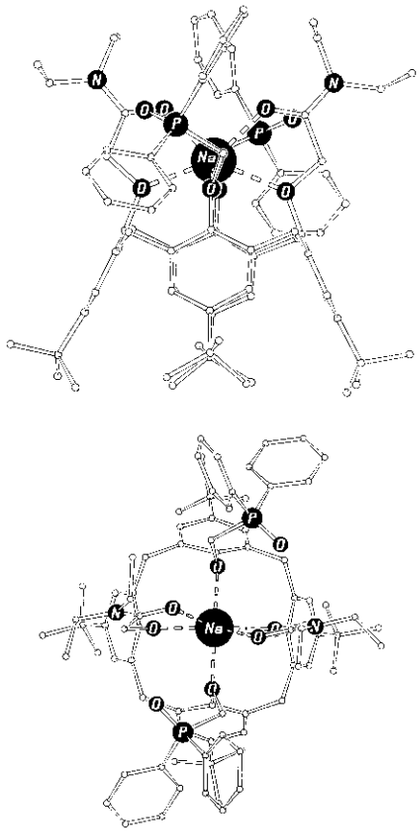

Fig. 6 Solid state structure of [**L1**·Na]BF_4. The BF_4 anion is not shown.

The average structure of the **L1**·Li^+ complex obtained by MD simulations is fully consistent with the experimentally determined NMR spectrum at −50 °C (Fig. 3a) and is of C_s symmetry. At room temperature both amide arms are competing for the Li^+ binding, which leads to the observed coalescence in the experimental NMR spectrum, due to an exchange between the bonded amide and the free one. As the simulated timescales are several orders of magnitude lower than the experimental one, we could only observe a stationary binding situation. Test calculations at 500 K in the gas phase showed an exchange of the two binding sites (Fig. 5), which might picture the dynamic exchange observed by NMR. The simulations for the **L2**·Li^+ system also result in a dissymmetric complex involving coordination of one phenolic oxygen and of three phosphoryl functions instead of four. However this conclusion could not be confirmed experimentally at temperatures above −70 °C. It is likely that the activation energy for Li migration between tripodal phosphoryl environments in **L2**·Li^+ is considerably lower than the one in **L1**·Li^+. This can be seen as a consequence of the equivalency of the binding arms, which generate four equivalent tripodal sites.

The observed Li movement between the two tetradentate binding units of M1 type constitutes a new example of ion migration within an organic backbone. Note, Li-jumps within an N_4-framework have recently been reported.[29] For the Li motion identified in the present work, the ion follows a curved pathway, as the transfer from one amide arm to the other is assisted by interaction with the two phenolic oxygens connected to the phosphoryl units.

Noteworthy is the difference in Li^+ *vs.* Na^+ binding modes by the two studied calixarenes in relation to their different hardness and coordination numbers. Li^+ may also form aggregates with anionic moieties of calixarenes[30,31] and generally achieves four to five coordination[32] while Na^+ may take up higher and more versatile coordination numbers.[33]

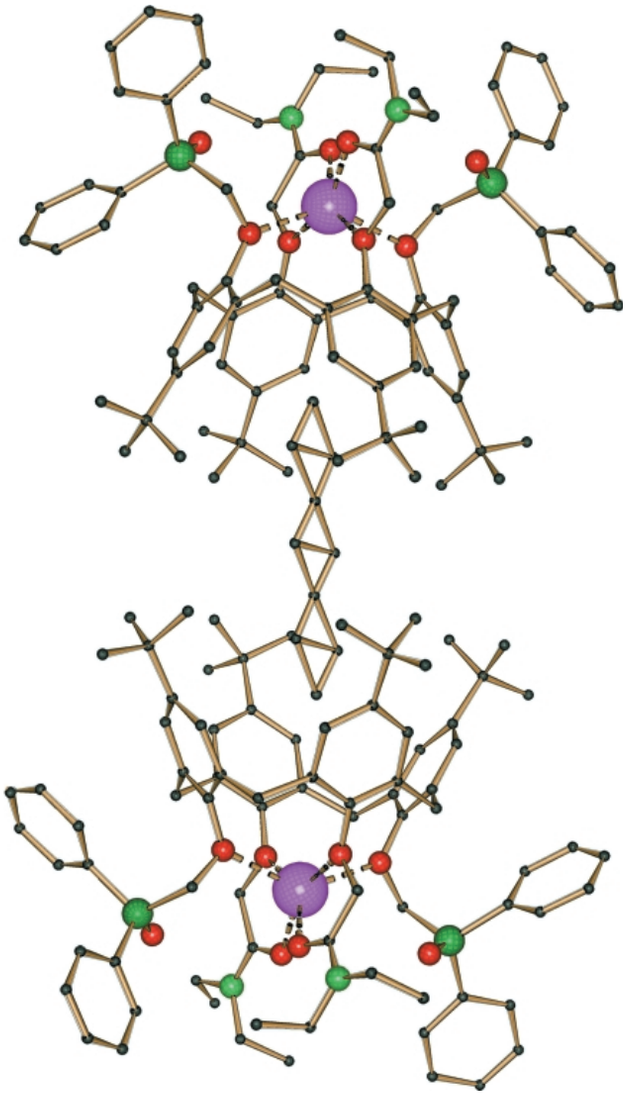

Fig. 7 Solid state structure of [**L1**·Na]BF_4 showing two calixarene units connected by a heptane molecule. The BF_4 anion is not shown.

Acknowledgements

Many thanks go to V. Berl, Dr P. N. W. Baxter and Dr R. G. Khoury for stimulating discussions and help concerning crystallization techniques and NMR procedures. CNRS-IDRIS and Université Louis Pasteur are acknowledged for computational facilities.

References

1 F. Arnaud-Neu, S. Fanni, L. Guerra, W. McGregor, K. Ziat, M. J. Schwing-Weill, G. Barrett, M. A. McKervey, D. Marrs and E. M. Seward, *J. Chem. Soc.*, *Perkin Trans. 2*, 1995, 113.

2 F. Arnaud-Neu, M.-J. Schwing-Weill, K. Ziat, S. Cremin, S. J. Harris and M. A. McKervey, *New J. Chem.*, 1991, **15**, 33.

3 F. Arnaud-Neu, S. Barboso, F. Berny, A. Casnati, N. Muzet, A. Pinalli, R. Ungaro, M. J. Schwing-Weil and G. Wipff, *J. Chem. Soc.*, *Perkin Trans. 2*, 1999, 1727.

4 A. F. D. de Namor, E. Gil, M. A. L. Tanco, D. A. P. Tanaka, L. E. P. Salazar, R. A. Schulz and J. Wang, *J. Phys. Chem.*, 1995, **99**, 16781.

5 A. F. D. de Namor, E. Gil, M. A. L. Tanco, D. A. P. Tanaka, L. E. P. Salazar, R. A. Schulz and J. Wang, *J. Phys. Chem.*, 1995, **99**, 16776.

6 A. F. D. de Namor, M. L. Zapata-Ormachea, O. Jafou and N. Al Rawi, *J. Phys. Chem. B*, 1997, **101**, 6772.

7 C. Wieser-Jeunesse, D. Matt, M. R. Yaftian, M. Burgard and J. M. Harrowfield, *C.R. Acad. Sci. Paris*, *t. 1*, *Sér. II*, 479.

8 M. R. Yaftian, M. Burgard, D. Matt, C. Wieser and C. Dieleman, *J. Inclusion Phenom.*, 1997, **27**, 127.

9 M. R. Yaftian, M. Burgard, A. El Bachiri, D. Matt, C. Wieser and C. Dieleman, *J. Inclusion Phenom.*, 1997, **29**, 137; M. R. Yaftian, M. Burgard, C. Wieser, C. B. Dieleman and D. Matt, *Solvent Extr. Ion Exch.*, 1998, 1131.

10 S. E. Matthews, M. Saadioui, V. Böhmer, S. Barboso, F. Arnaud-Neu, M.-J. Schwing-Weill, A. G. Carrera and J.-F. Dozol, *J. Prakt. Chem.*, 1999, **241**, 264; J. F. Malone, D. J. Marrs, A. McKervey, P. O'Hagan, N. Thompson, A. Walker, F. Arnaud-Neu, O. Mauprivez, M.-J. Schwing, J.-F. Dozol, H. Rouquette and N. Simon, *J. Chem. Soc.*, *Chem. Commun.*, 1995, 2151; F. Arnaud-Neu, J. K. Browne, D. Byrne, D. J. Marrs, M. A. McKervey, P. O'Hagan, M.-J. Schwing-Weill and A. Walker, *Chem. Eur. J.*, 1999, **5**, 175; S. Barboso, A. G. Carrera, S. E. Matthews, F. Arnaud-Neu, V. Böhmer, J.-F. Dozol, H. Rouquette and M.-J. Schwing-Weill, *J. Chem. Soc.*, *Perkin Trans. 2*, 1999, 719.

11 L. Le Saulnier, S. Varbanov, R. Scopelliti, M. Elhabiri and J.-C. G. Bünzli, *J. Chem. Soc.*, *Dalton Trans.*, 1999, 3919.

12 A. McKervey, M.-J. Schwing and F. Arnaud-Neu, in *Comprehensive Supramolecular Chemistry*, J. L. Atwood, J. E. D. Davies, D. D. McNicol, F. Vögtle and J.-M. Lehn Ed., Pergamon, New York, 1996, pp. 537–603.

13 A. Arduini, E. Ghidini, A. Pochini, R. Ungaro, G. D. Andreetti, G. Calestani and F. Ugozzoli, *J. Inclusion Phenom.*, 1988, **6**, 119.

14 G. Calestani, F. Ugozzoli, A. Arduini, E. Ghidini and R. Ungaro, *J. Chem. Soc.*, *Chem. Commun.*, 1987, 344.

15 P. Guilbaud, A. Varnek and G. Wipff, *J. Am. Chem. Soc.*, 1993, **115**, 8298; A. Varnek and G. Wipff, *J. Phys. Chem.*, 1993, **97**, 10840.

16 OPenMoleN, Interactive Structure Solution, Nonius B.V., Delft, 1997.

17 D. A. Pearlman, D. A. Case, J. C. Caldwell, W. S. Ross, T. E. Cheatham III, D. M. Ferguson, G. L. Seibel, U. C. Singh, P. Weiner and P. A. Kollman, AMBER4.1, 1995.

18 E. Engler and G. Wipff, unpublished results.

19 E. Engler and G. Wipff, in *Crystallography of Supramolecular Compounds*, G. Tsoucaris, Ed., Kluwer, Dordrecht, 1996, pp. 471–476.

20 W. D. Cornell, P. Cieplak, C. I. Bayly, I. R. Gould, K. M. Merz, D. M. Ferguson, D. C. Spellmeyer, T. Fox, J. W. Caldwell and P. A. Kollman, *J. Am. Chem. Soc.*, 1995, **117**, 5179.

21 N. Muzet, G. Wipff, A. Casnati, L. Domiano, R. Ungaro and F. Ugozzoli, *J. Chem. Soc.*, *Perkin Trans. 2*, 1996, 1065.

22 S. Fischer, P. D. J. Grootenhuis, L. C. Groenen, W. P. van Horn, F. C. J. M. van Veggel, D. N. Reinhoudt and M. Karplus, *J. Am. Chem. Soc.*, 1995, **117**, 1611.

23 SPARTAN version 4.0.4., Wavefunction Inc., Irvine, USA, 1995.

24 J. Åqvist, *J. Phys. Chem.*, 1990, **94**, 8021.

25 H. Günther, in *NMR-Spektroskopie*, Thieme, Stuttgart, 1992, p. 310.

26 M. Perrin and D. Oehler, in *Calixarenes*, J. Vicens and V. Böhmer, Ed., Kluwer, Dordrecht, 1991, pp. 65–85.

27 C. Dieleman, C. Loeber, D. Matt, A. De Cian and J. Fischer, *J. Chem. Soc.*, *Dalton Trans.*, 1995, 3097.

28 F. Berny, N. Muzet, L. Troxler, A. Dedieu and G. Wipff, *Inorg. Chem.*, 1999, **38**, 1244.

29 M. Veith, M. Zimmer, K. Fries, J. Böhnlein-Maus and V. Huch, *Angew. Chem.*, *Int. Ed.*, 1996, **35**, 1529.

30 M. G. Davison, J. A. K. Howard, S. Lamb and C. W. Lehman, *Chem. Commun.*, 1997, 1607.

31 F. Hamada, K. D. Robinson, G. W. Orr and J. L. Atwood, *Supramol. Chem.*, 1993, **2**, 19.

32 U. Olsher, R. M. Izatt, J. S. Bradshow and N. K. Dalley, *Chem. Rev.*, 1991, **91**, 137.

33 P. Chakrabarti, K. Venkatesan and C. N. R. Rao, *Proc. R. Soc. London*, *Ser. A*, 1981, **375**, 127.